

GENETICS

Correction of diverse muscular dystrophy mutations in human engineered heart muscle by single-site genome editing

Chengzu Long,^{1,2,3,4,*†} Hui Li,^{1,2,3,*} Malte Tiburcy,^{5,6} Cristina Rodriguez-Caycedo,^{1,2,3} Viktoriia Kyrychenko,^{1,2,3} Huanyu Zhou,^{1,2,3} Yu Zhang,^{1,2,3} Yi-Li Min,^{1,2,3} John M. Shelton,⁷ Pradeep P. A. Mammen,^{2,3,7} Norman Y. Liaw,⁵ Wolfram-Hubertus Zimmermann,^{5,6} Rhonda Bassel-Duby,^{1,2,3} Jay W. Schneider,^{2,3,7} Eric N. Olson^{1,2,3†}

Copyright © 2018
The Authors, some
rights reserved;
exclusive licensee
American Association
for the Advancement
of Science. No claim to
original U.S. Government
Works. Distributed
under a Creative
Commons Attribution
NonCommercial
License 4.0 (CC BY-NC).

Genome editing with CRISPR/Cas9 is a promising new approach for correcting or mitigating disease-causing mutations. Duchenne muscular dystrophy (DMD) is associated with lethal degeneration of cardiac and skeletal muscle caused by more than 3000 different mutations in the X-linked dystrophin gene (*DMD*). Most of these mutations are clustered in “hotspots.” There is a fortuitous correspondence between the eukaryotic splice acceptor and splice donor sequences and the protospacer adjacent motif sequences that govern prokaryotic CRISPR/Cas9 target gene recognition and cleavage. Taking advantage of this correspondence, we screened for optimal guide RNAs capable of introducing insertion/deletion (indel) mutations by nonhomologous end joining that abolish conserved RNA splice sites in 12 exons that potentially allow skipping of the most common mutant or out-of-frame *DMD* exons within or nearby mutational hotspots. We refer to the correction of *DMD* mutations by exon skipping as myoediting. In proof-of-concept studies, we performed myoediting in representative induced pluripotent stem cells from multiple patients with large deletions, point mutations, or duplications within the *DMD* gene and efficiently restored dystrophin protein expression in derivative cardiomyocytes. In three-dimensional engineered heart muscle (EHM), myoediting of *DMD* mutations restored dystrophin expression and the corresponding mechanical force of contraction. Correcting only a subset of cardiomyocytes (30 to 50%) was sufficient to rescue the mutant EHM phenotype to near-normal control levels. We conclude that abolishing conserved RNA splicing acceptor/donor sites and directing the splicing machinery to skip mutant or out-of-frame exons through myoediting allow correction of the cardiac abnormalities associated with *DMD* by eliminating the underlying genetic basis of the disease.

INTRODUCTION

Duchenne muscular dystrophy (*DMD*) afflicts ~1 in 5000 males (1) and is caused by mutations in the X-linked dystrophin gene (*DMD*). These mutations include large deletions, large duplications, point mutations, and other small mutations. The rod-shaped dystrophin protein links the cytoskeleton and the extracellular matrix of muscle cells and maintains the integrity of the plasma membrane (2). In its absence, muscle cells degenerate. Although *DMD* causes many severe symptoms, dilated cardiomyopathy (*DCM*) is a leading cause of death of *DMD* patients (3), and there is no curative treatment for *DMD* thus far.

CRISPR (clustered regularly interspaced short palindromic repeats)/Cas9 (CRISPR-associated protein 9)-mediated genome editing is emerging as a promising tool for correction of genetic disorders (4–6). Briefly, an engineered RNA-guided nuclease, Cas9 or Cpf1 (7), generates a double-strand break (DSB) at the targeted genomic locus adjacent to

a short protospacer adjacent motif (PAM) sequence. There are three primary pathways to repair the DSB (8): (i) Nonhomologous end joining (NHEJ) directly ligates two DNA ends and leads to imprecise insertion/deletion (indel) mutations. (ii) Homology-directed repair (HDR) uses sister chromatid or exogenous DNA as a repair template and generates a precise modification at the target sites. (iii) Microhomology-mediated end joining (MMEJ) uses short sequences of nucleotide homology (5 to 25 base pairs) flanking the original DSB to ligate the broken ends and deletes the region between the microhomologies. Although NHEJ can effectively generate indel mutations in most cell types, HDR- or MMEJ-mediated editing is generally thought to be restricted to proliferating cells.

We and others have used CRISPR/Cas9-mediated genome editing to correct the *Dmd* point mutation in the germ line (9) or muscle stem cells (10) of *mdx* mice, via HDR, and in the postnatal muscle tissue of this mouse by NHEJ (11–13). However, correction of this point mutation does not fully address whether genome editing is applicable across the heterogeneous spectrum of mutations that cause *DMD* in humans. Most of *DMD* patients harbor deletions in one or more exons, whereas only 5 to 9% of *DMD* patients have point mutations.

Internal in-frame deletions of dystrophin are associated with Becker muscular dystrophy (BMD), a relatively mild form of muscular dystrophy. Inspired by the attenuated clinical severity of BMD versus *DMD*, exon skipping has been advanced as a therapeutic strategy to bypass mutations that disrupt the dystrophin open reading frame by modulating splicing patterns of the *DMD* gene (14). Several recent studies used CRISPR/Cas9-mediated genome editing to correct various types of

¹Department of Molecular Biology, University of Texas Southwestern Medical Center, Dallas, TX 75390, USA. ²Senator Paul D. Wellstone Muscular Dystrophy Cooperative Research Center, University of Texas Southwestern Medical Center, Dallas, TX 75390, USA. ³Hamon Center for Regenerative Science and Medicine, University of Texas Southwestern Medical Center, Dallas, TX 75390, USA. ⁴Leon H. Charney Division of Cardiology, New York University School of Medicine, New York, NY 10016, USA. ⁵Institute of Pharmacology and Toxicology, University Medical Center, Georg-August-University Göttingen, Göttingen, 37075, Germany. ⁶DZHK (German Center for Cardiovascular Research), partner site Göttingen, Göttingen, Germany. ⁷Department of Internal Medicine, University of Texas Southwestern Medical Center, Dallas, TX 75390, USA.

*These authors contributed equally to this work.

†Corresponding author. Email: eric.olson@utsouthwestern.edu (E.N.O.); chengzu.long@nyumc.org (C.L.)

DMD mutations in human cells and mice (10, 15–28). Some have deployed pairs of guide RNAs to correct the mutation, which requires simultaneous cutting of DNA and excision of large intervening genomic sequences (23 to 725 kb). Fortunately, the PAM sequence for *Streptococcus pyogenes* Cas9 (SpCas9), the first and most widely used form of Cas9, contains NAG or NGG, corresponding to the universal splice acceptor sequence (AG) and most of the donor sequences (GG). Thus, in principle, directing Cas9 to splice junctions and the elimination of these consensus sequences by indels can allow for efficient exon skipping. In addition, only a single cleavage of DNA, which disrupts the splice site, can enable skipping of an entire exon.

Given the thousands of individual DMD mutations that have been identified in humans, an obvious question is how such a large number of mutations might be corrected by CRISPR/Cas9-mediated genome editing. Human DMD mutations are clustered in specific “hotspot” areas of the gene (exons 45 to 55 and exons 2 to 10) (29) such that skipping 1 or 2 of 12 targeted exons within or nearby the hotspots (termed “top 12 exons”) can, in principle, rescue dystrophin function in a majority (~60%) of DMD patients (30). Here, we used CRISPR/Cas9 with single-guide RNAs to destroy the conserved splice acceptor or donor sites preceding DMD mutations or to bypass mutant or out-of-frame exons, thereby allowing splicing between surrounding exons to recreate in-frame dystrophin proteins lacking the mutations. We first tested this approach by screening for optimal guide RNAs capable of inducing skipping of the *DMD* 12 exons that would potentially allow skipping of the most commonly mutated or out-of-frame exons within nearby mutational hotspots. As examples of this approach, we demonstrate the restoration of dystrophin expression in induced pluripotent stem cell (iPSC)-derived cardiomyocytes harboring exon deletions and a pseudo-exon point mutation. Finally, we used human iPSC-derived three-dimensional (3D) engineered heart muscle (EHM) to test the efficacy of gene editing to overcome abnormalities in cardiac contractility associated with DMD. Contractile dysfunction was observed in DMD EHM, recapitulating the DCM clinical phenotype of DMD patients, and contractile function was effectively restored in corrected DMD EHM. We conclude that genome editing represents a potentially powerful means of eliminating the genetic cause and correcting the muscle and cardiac abnormalities associated with DMD.

RESULTS

Identification of optimal guide RNAs to target 12 different exons associated with hotspot regions of DMD mutations

A list of the top 12 exons that, when skipped, can potentially restore the dystrophin open reading frame in most of the hotspot regions of DMD mutations is shown in Table 1. As an initial step toward correcting a majority of human DMD mutations by exon skipping, we screened pools of guide RNAs to target the top 12 exons of the human *DMD* gene (Fig. 1, A and B). We selected three to six PAM sequences (NAG or NGG) to target the 3' or 5' splice sites, respectively, of each exon (Fig. 1A and Table 1). These guide RNAs were cloned in plasmid SpCas9-2A-GFP, as described previously (9). Indels that remove essential splice donor or acceptor sequences allow for skipping of the corresponding target exon. On the basis of the frequency of known DMD mutations, these guide RNAs would be predicted to be capable of rescuing dystrophin function in up to 60% of DMD patients (30).

To test the feasibility and efficacy of this strategy in the human genome, we initially used human embryonic kidney 293 cells (293 cells) to target the splice acceptor site of exon 51 (Fig. 1C). Transfected 293 cells

were sorted by green fluorescent protein (GFP) expression, and gene editing efficiency was detected by the mismatch-specific T7E1 endonuclease assay, as described previously (fig. S2A) (9). The ability of three guide RNAs (Ex51-g1, Ex51-g2, and Ex51-g3) to target the splice acceptor site of exon 51 is shown in Table 1 and Fig. 2B. In GFP-positive sorted 293 cells, Ex51-g3 showed high editing activity, whereas Ex51-g1 and Ex51-g2 had no detectable activity. These results highlight the importance of optimization of guide RNA sequences. Next, we evaluated the cleavage efficiency of guide RNAs, which target the top 12 exons, including exons 51, 45, 53, 44, 46, 52, 50, 43, 6, 7, 8, and 55. One or two guide RNAs with the highest efficiency of editing of each exon are shown in Fig. 1C. The selected guide RNAs for exons 51, 45, and 55 use NAG as the PAM (Table 1). Genomic polymerase chain reaction (PCR) products from the myoedited top 12 exons were cloned and sequenced, as described previously (fig. S1A and table S1) (25). We observed indels that removed essential splice sites or shifted the open reading frame (fig. S1A). In brain and kidney tissues, an N-terminally truncated form of dystrophin (Dp140) is transcribed from an alternative promoter in intron 44 (31). Skipping of six targeted exons (exons 51, 53, 46, 52, 50, and 55) in Dp140 mRNA was confirmed in 293 cells by sequencing of reverse transcription PCR (RT-PCR) products (fig. S1B).

Correction of diverse DMD patient mutations by myoediting

To evaluate the effectiveness of a single-guide RNA to correct different types of human DMD mutations by exon skipping, we obtained or generated three DMD iPSC lines with representative types of DMD mutations: a large deletion (termed Del; lacking exons 48 to 50), a pseudo-exon mutation (termed pEx; caused by an intronic point mutation), and a duplication mutation (termed Dup). Briefly, peripheral blood mononuclear cells (PBMCs) obtained from whole blood were cultured and then reprogrammed into iPSCs using recombinant Sendai viral vectors expressing reprogramming factors (15). Cas9 and guide RNAs for correction or bypass of the mutations in iPSC lines were introduced into cells by nucleofection, as described previously (25). Pools of treated cells or single clones were then differentiated into induced cardiomyocytes (iCMs) using standardized conditions (25, 32). Purified iCMs were used to generate 3D-EHM and to perform functional assays (Fig. 2A).

Correction of a large deletion mutation

It is estimated that ~60 to 70% of DMD cases are caused by large deletions of one or more exons. We performed myoediting on an iPSC line from a DMD patient with a large deletion of exons 48 to 50 in a hotspot, which creates a frameshift mutation and introduces a premature stop codon in exon 51, as shown in Fig. 2B. Destruction of the splice acceptor in exon 51 will, in principle, allow for splicing of exon 47 to exon 52, thereby reconstituting the open reading frame (Fig. 2B and fig. S2B). Theoretically, skipping exon 51 can potentially correct ~13% of DMD patients (30). Optimized guide RNA Ex51-g3 and Cas9 (Fig. 2C) were nucleofected into this iPSC line, resulting in successful destruction of the splice acceptor or reframing of exon 51 by NHEJ, as demonstrated by genomic sequencing, and restoration of the open reading frame (fig. S2B). We differentiated the pool of myoedited and DMD iPSCs (Del-Cor.) into iCMs and confirmed rescue of in-frame dystrophin mRNA expression by sequencing of RT-PCR products from amplification of exons 47 to 52 (Fig. 2D and fig. S2C).

Correction of a pseudo-exon mutation

To further extend this approach to rare mutations, we attempted to correct a point mutation within iPSCs from a DMD patient who has a

Table 1. Guide RNA sequences of top 12 exons.

Exon	Applicability (30)	gRNA/PAM at acceptor site	gRNA/PAM at donor site
51	13.0%	#1: TGCAAAAACCCAAAATATTTTAG	
		#2: AAAATATTTAGCTCCTACTCAG	
		#3: CAGAGTAACAGTCTGAGTAGGAG*	
45	8.1%	#1: TTGCCTTTTGGTATCTTACAGG	
		#2: TTTGCCTTTTGGTATCTTACAG	
		#3: CGCTGCCCAATGCCATCCTGGAG	
53	7.7%	#1: ATTTATTTTCTTTTATTCTAG	#4: AAAGAAAATCACAGAAACCAAGG
		#2: TTTCTTTTATTCTAGTTGAAAG	#5: AAAATCACAGAAACCAAGGTTAG
		#3: TGATTCTGAATTCTTCAACTAG	#6: GGTATCTTTGATACTAACCTTGG
44	6.2%	#1: ATCCATATGCTTTTACCTGCAGG	#4: GTAATACAAATGGTATCTTAAGG
		#2: GATCCATATGCTTTTACCTGCAG	
		#3: CAGATCTGTCAAATCGCCTGCAG	
46	4.3%	#1: TTATTCTTCTTCTCCAGGCTAG	
		#2: AATTTTATTCTTCTTCTCCAGG	
		#3: CAATTTTATTCTTCTTCTCCAG	
52	4.1%	#1: TAAGGGATATTTGTTCTTACAGG	
		#2: CTAAGGGATATTTGTTCTTACAG	
		#3: TGTCTTACAGGCAACAATGCAG	
50	4.0%	#1: TGTATGCTTTTCTGTTAAAGAGG	
		#2: ATGTGTATGCTTTTCTGTTAAAG	
		#3: GTGTATGCTTTTCTGTTAAAGAG	
43	3.8%	#1: GTTTTAAAATTTTATATTACAG	#4: TATGTGTTACCTACCCTTGTCCGG
		#2: TTTTATATTACAGAATATAAAAG	#5: AAATGTACAAGGACCGACAAGGG
		#3: ATATTACAGAATATAAAAGATAG	#6: GTACAAGGACCGACAAGGGTAGG
6	3.0%†	#1: TGAAAATTTATTTCCACATGTAG	#4: ATGCTCTCATCCATAGTCATAGG
		#2: GAAAATTTATTTCCACATGTAGG	#5: TCTCATCCATAGTCATAGGTAAG
		#3: TTACATTTTGGACCTACATGTGG	#6: CATCCATAGTCATAGGTAAGAAG
7	3.0%†	#1: TGTGTATGTGTATGTGTTTTAGG	
		#2: TATGTGTATGTGTTTTAGGCCAG	
		#3: CTATTCCAGTCAAATAGGTCTGG	
8	2.3%	#1: GTGTAGTGTTAATGTGCTTACAG	#4: TGCACTATTCTCAACAGGTAAG
		#2: GGACTTCTTATCTGGATAGGTGG	#5: TCAAATGCACTATTCTCAACAGG
		#3: TAGGTGGTATCAACATCTGTAAG	#6: CTTTACACACTTTACCTGTTGAG
55	2.0%	#1: TGAACATTTGGTCTTTGCAGGG	
		#2: TCTGAACATTTGGTCTTTGCAG	
		#3: TCTCGCTCACTACCTGCAAAG	

*Bold sequence indicates the best guide RNAs for myoediting. †Dual exon skipping (exons 6 and 7).

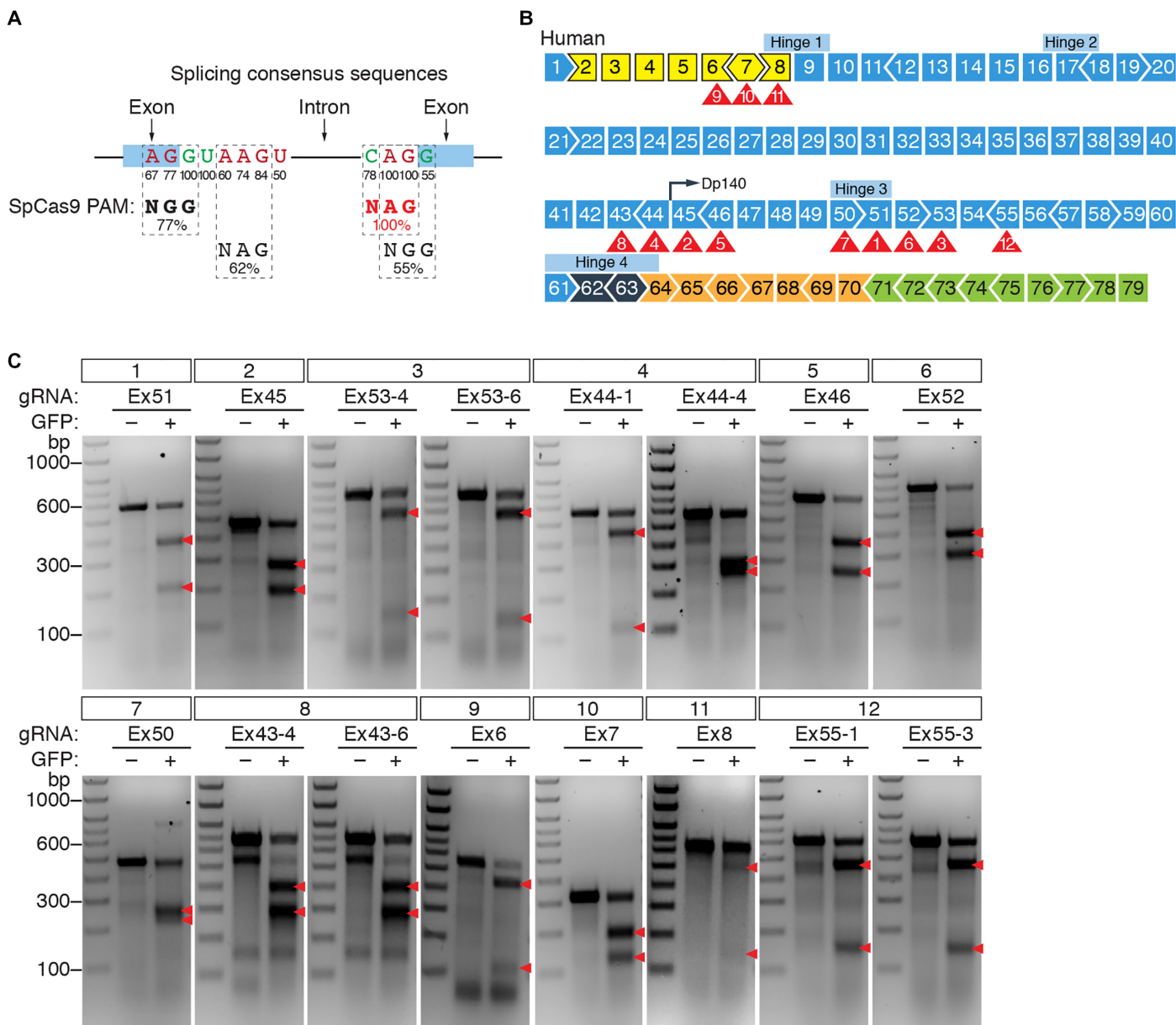


Fig. 1. Myoediting strategy and identification of optimal guide RNAs to target the top 12 exons in DMD. (A) Conserved splice sites contain multiple NAG and NGG sequences, which enable cleavage by SpCas9. The numbers indicate the frequency of occurrence (%). (B) Human *DMD* exon structure. Shapes of intron-exon junctions indicate complementarity that maintains the open reading frame upon splicing. Red arrowheads indicate the top 12 targeted exons. The numbers indicate the order of the exons. (C) T7E1 assays in human 293 cells transfected with plasmids expressing the corresponding guide RNA (gRNA), SpCas9, and GFP for the top 12 exons. The PCR products from GFP⁺ and GFP⁻ cells were cut with T7 endonuclease I (T7E1), which is specific to heteroduplex DNA caused by CRISPR/Cas9-mediated genome editing. Red arrowhead indicates cleavage bands of T7E1. bp indicates the base pair length of the marker bands.

spontaneous point mutation in intron 47 (c.6913-4037T>G). This point mutation generates a novel RNA splicing acceptor site (YnNYAG) and results in a pseudo-exon of exon 47A (Fig. 2E), which encodes a premature stop signal (33). We designed two guide RNAs (Ex47A-g1 and Ex47A-g2) to precisely target the mutation (Fig. 2F and fig. S3, A and B). As shown in Fig. 2G, myoediting abolished the cryptic splice acceptor site and permanently skipped the pseudo-exon, restoring full-length dystrophin protein in the corrected cells (pEx-Cor.). We tested the efficacy of exon skipping by RT-PCR in these DMD iCMs (Fig. 2G). Sequencing of the RT-PCR products confirmed that exon 47 was spliced to exon 48 (fig. S3C).

It is noteworthy that Ex47A-g2 targets only the mutant allele because the wild-type intron lacks the PAM sequence (NAG) for SpCas9. Moreover, the T > G mutation in this patient creates a disease-specific PAM sequence (AG) for Cas9. It is also noteworthy that this type of correction restores the normal dystrophin protein without any internal deletions (fig. S3, B and C).

Correction of a large duplication mutation

Exon duplications account for ~10 to 15% of identified DMD-causing mutations. We tested myoediting on an iPSC line (also known as Dup) from a DMD patient with a large duplication (exons 55 to 59), which

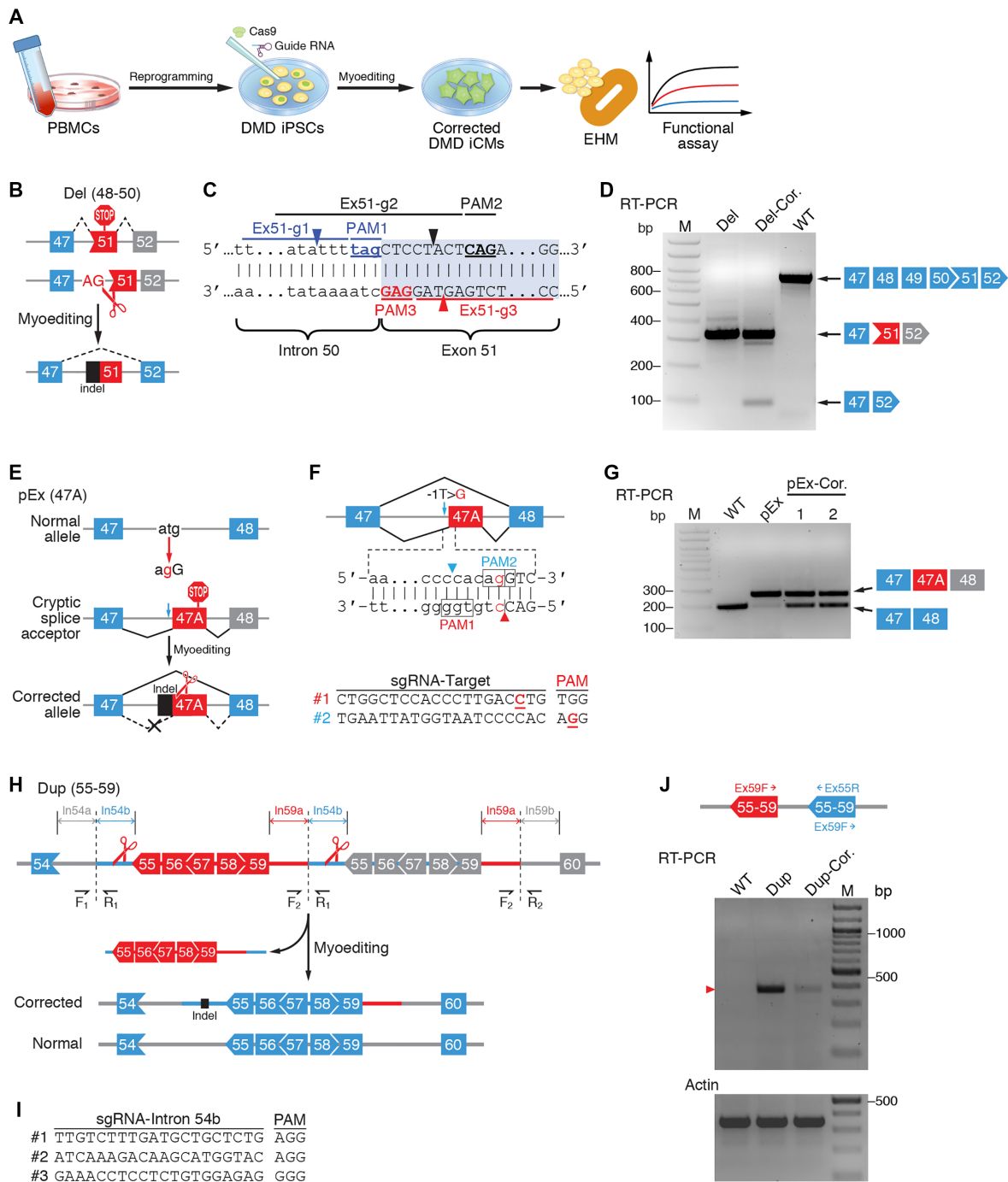


Fig. 2. Rescue of dystrophin mRNA expression in iPSC-derived cardiomyocytes with diverse mutations by myoeediting. (A) Schematic of the myoeediting of DMD iPSCs and 3D-EHMs-based functional assay. (B) Myoeediting targets the exon 51 splice acceptor site in Del DMD iPSCs. A deletion (exons 48 to 50) in a DMD patient creates a frameshift mutation in exon 51. The red box indicates out-of-frame exon 51 with a stop codon. Destruction of the exon 51 splice acceptor in DMD iPSCs allows splicing from exons 47 to 52 and restoration of the dystrophin open reading frame. (C) Using the guide RNA library, three guide RNAs (Ex51-g1, Ex51-g2, and Ex51-g3) that target sequences 5' of exon 51 were selected. (D) RT-PCR of cardiomyocytes differentiated from uncorrected DMD (Del), corrected DMD (Del-Cor.), and WT iPSCs. Skipping of exon 51 allows splicing from exons 47 to 52 (lower band) and restoration of the *DMD* open reading frame. (E) Myoeediting strategy for pseudo-exon 47A (pEx). *DMD* exons are represented as blue boxes. Pseudo-exon 47A (red) with stop codon is marked by a stop sign. The black box indicates myoeediting-mediated indel. (F) Sequence of guide RNAs for pseudo-exon 47A of pEx. *DMD* exons are represented as blue boxes, and pseudo-exons are represented as red boxes (47A). sgRNA, single-guide RNA. (G) RT-PCR of human cardiomyocytes differentiated from WT, uncorrected DMD (pEx), and corrected DMD iPSCs (pEx-Cor.) by guide RNAs In47A-g1 and In47A-g2. Skipping of pseudo-exon 47A allows splicing from exons 47 to 48 (lower band) and restoration of the *DMD* open reading frame. (H) Myoeediting strategy for the duplication (Dup) of exons 55 to 59. *DMD* exons are represented as blue boxes. Duplicated exons are represented as red boxes. The black box indicates myoeediting-mediated indel. (I) Sequence of guide RNAs for intron 54 of Dup (In54-g1, In54-g2, and In54-g3). (J) RT-PCR of human cardiomyocytes differentiated from WT, uncorrected DMD (Dup), and corrected DMD iPSCs (Dup-Cor.). Skipping of duplicated exons 55 to 59 allows splicing from exons 54 to 55 and restoration of the *DMD* open reading frame. RT-PCR of RNA was performed with the indicated sets of primers (F and R) (table S2).

disrupts the dystrophin open reading frame (Fig. 2H). We performed whole-genome sequencing and analyzed the copy number variation profile in cells from this patient and identified the precise insertion site in intron 54 (Fig. 2H). This insertion site (In59-In54 junction) was confirmed by PCR (fig. S4A and table S2).

We hypothesized that the 5' flanking sequence of the duplicated exon 55 is identical such that one guide RNA targeting this region should be able to make two DSBs and delete the entire duplicated region (exons 55 to 59; ~150 kb). To test this hypothesis, we designed three guide RNAs (In54-g1, In54-g2, and In54-g3) against sequences near the junction of intron 54 and exon 55 (Fig. 2I). The efficiency of DNA cutting with these guide RNAs was evaluated in 293 cells by T7E1 (fig. S4B). Guide RNA In54-g1 was selected for subsequent experiments on Dup iPSCs. Genomic PCR products from the myoedited Dup iPSC mixture were cloned and sequenced, as described previously (fig. S4C) (25).

To confirm the correction of the duplication mutation, we differentiated the pool of treated DMD iPSCs (also known as Dup-Cor.) into cardiomyocytes. mRNA with duplicated exons was semiquantified by RT-PCR using the duplication-specific primers (Ex59F, a forward primer in exon 59, and Ex55R, a reverse primer in exon 55) and normalized to expression of the β -actin gene (Fig. 2J and table S2). As expected, the duplication-specific RT-PCR band was absent in wild-type (WT) cells and was decreased dramatically in Dup-Cor. cells. To confirm this result, we performed RT-PCR on the duplication borders of exon 53 to Ex55 and Ex59 to exon 60 (fig. S4D). The intensity of duplication-specific upper bands was decreased in corrected iCMs. Single colonies were picked from the treated mixture of cells. Duplication-specific PCR primers (F2-R1) were used to screen the corrected colonies (fig. S4E). PCR results of three representative corrected colonies (Dup-Cor. #4, #6, and #26) and the uncorrected control (Dup) are shown in fig. S4E. The absence of a duplication-specific PCR band in colonies 4, 6, and 26 confirmed the deletion of the duplicated DNA region.

Restoration of dystrophin protein in patient-derived iCMs by myoediting

Next, we confirmed the restoration and stable expression of dystrophin protein in single clones and pools of treated iCMs and by immunocytochemistry (Fig. 3, A to C, and figs. S2D, S3D, and S4F) and Western blot analysis (Fig. 3, D to F, and fig. S5). Even without clonal selection and expansion, most of the iCMs in Del-Cor., pEx-Cor., and Dup-Cor. were dystrophin-positive (Fig. 3, A to C, and figs. S2D, S3D, and S4F). From mixtures of myoedited Del iPSCs, we picked two clones (#16 and #27) and differentiated the single clones into cardiomyocytes (fig. S5A and table S3). Clone #27, which has a higher dystrophin expression level, was selected for subsequent experiments (also known as Del-Cor-SC). One selected clone for corrected pEx (#19) is presented in fig. S5B and was used for further studies (also known as pEx-Cor-SC). Two selected clones for corrected Dup (#26 and #6) were differentiated into iCMs (fig. S5C). Clone #6 was used for functional assay experiments (also known as Dup-Cor-SC). Dystrophin protein expression levels of the corrected iCMs were estimated to be comparable to WT cardiomyocytes (50 to 100%) by immunocytochemistry and Western blot analysis (Fig. 3 and fig. S5).

Restoration of function of patient-derived iCMs by myoediting

In addition to measuring dystrophin mRNA and protein expression by biochemical methods, we used functional analysis to the macroscale using 3D-EHM derived from normal, DMD, and corrected DMD

iCMs, as described previously (32). Briefly, iPSCs-derived cardiomyocytes were metabolically purified by glucose deprivation (fig. S6). Purified cardiomyocytes were mixed with human foreskin fibroblasts (HFFs) at a 70%:30% ratio. The cell mixture was reconstituted in a mixture of bovine collagen and serum-free medium. After 4 weeks in culture, contraction experiments were performed (Fig. 4A).

We tested EHM from eight iPSC lines: (i) WT, (ii) uncorrected Del, (iii) Del-Cor-SC, (iv) uncorrected pEx, (v) pEx-Cor., (vi) pEx-Cor-SC, (vii) uncorrected Dup, and (viii) Dup-Cor-SC. Functional phenotyping of DMD and corrected DMD cardiomyocytes in EHM revealed a contractile dysfunction in all DMD EHM (Del, pEx, and Dup) compared to WT EHM (Fig. 4, B to E, and movies S1 to S8). A more pronounced contractile dysfunction was seen in Del compared with pEx and Dup EHM. Force of contraction (FOC) was markedly reduced in DMD EHM and was significantly improved in corrected DMD EHM (Del-Cor-SC, pEx-Cor-SC, and Dup-Cor-SC) (Fig. 4, B to E) with completely restored cardiomyocyte maximal inotropic capacity in Dup-Cor-SC (Fig. 4, D and E).

Because current gene therapy delivery methods are only able to affect a portion of the heart muscle, an obvious question is what percentage of corrected cardiomyocytes is needed to rescue the phenotype of DCM. To address this question, we precisely mixed DMD cells (Del) and corrected DMD cells (Del-Cor-SC) to simulate a wide range of "therapeutic efficiency" (10 to 100%) in EHM (Fig. 4F). This revealed that 30 to 50% of cardiomyocytes need to be repaired for partial (30%) or maximal (50%) rescue of the contractile phenotype (Fig. 4F). These findings are consistent with previous *in vivo* studies (34) showing that mosaic dystrophin expression in 50% cardiomyocytes in carrier mice resulted in a near-normal cardiac phenotype. Our findings show that contractile dysfunction was efficiently restored in corrected DMD EHM to a comparable level of WT EHM. Myoediting is thus a highly specific and efficient approach to rescue clinical phenotypes of DMD in EHM.

DISCUSSION

The *DMD* gene is the largest known gene in the human genome, encompassing 2.6 million base pairs and encoding 79 exons. The large size and complicated structure of the *DMD* gene contribute to its high rate of spontaneous mutation. There are ~3000 documented mutations in humans, which include large deletions or duplications (~77%), small indels (~12%), and point mutations (~9%). These mutations mainly affect exons; however, intronic mutations can alter the splicing pattern and cause the disease, as shown here for the pEx mutation.

In an effort to collectively correct multiple hotspot mutations in the human genome, Ousterout *et al.* (17) deleted the entire 336-kb genomic region flanking exons 45 to 55 in human DMD myoblasts by multiplexed guide RNAs targeting introns 44 and 55. Similarly, a larger 725-kb deletion from introns 44 to 55 was shown to restore the dystrophin open reading frame in multiple DMD patient-derived iPSCs, which contain mutations in this region (16). Bengtsson *et al.* (24) also targeted introns 51 and 53 and removed exons 52 and 53 in the *mdx*^{4cv} mouse model. The premature termination codon in exon 23 of *mdx* and *mdx/Utr*^{+/-} mice was also bypassed by removing a 23-kb genomic region encompassing multiple exons (exons 21 to 23) (19, 27).

To potentially simplify the correction of diverse DMD mutations by CRISPR/Cas9 gene editing, we identified guide RNAs capable of skipping the top 12 exons, which account for ~60% of DMD patients. Thus, it is not necessary to design individual guides for each DMD mutation or excise large genomic regions with pairs of guide RNAs.

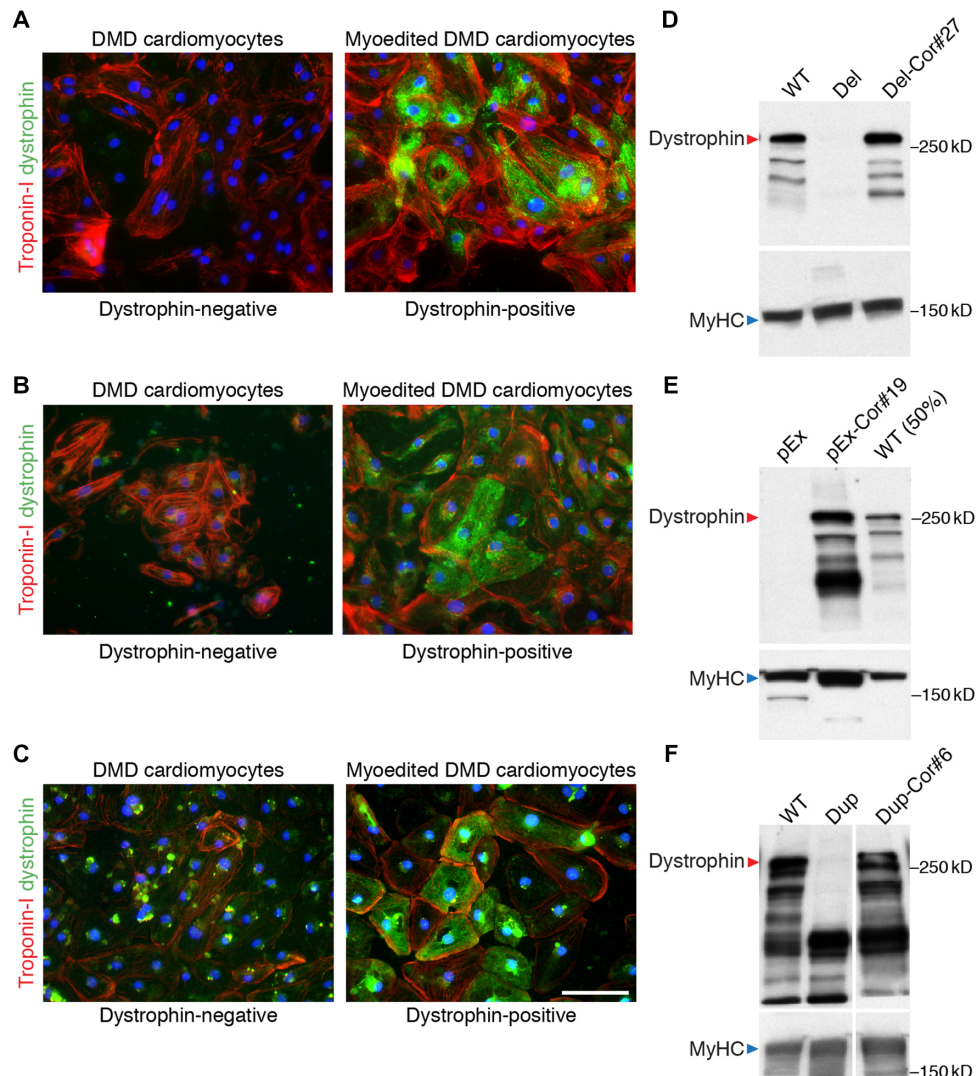


Fig. 3. Immunocytochemistry and Western blot analysis show dystrophin protein expression rescued by myoediting. (A to C) Immunocytochemistry of dystrophin expression (green) shows DMD iPSC cardiomyocytes lacking dystrophin expression. Following successful myoediting, the corrected DMD iPSC cardiomyocytes express dystrophin. Immunofluorescence (red) detects cardiac marker troponin-I. Nuclei are labeled by Hoechst dye (blue). (D to F) Western blot analysis of WT (100 and 50%), uncorrected (Del, pEx, and Dup) and corrected DMD (Del-Cor#27, pEx-Cor#19, and Dup-Cor#6) iCM. Red arrowhead (above 250 kD) indicates the immunoreactive bands of dystrophin. Blue arrowhead (above 150 kD) indicates the immunoreactive bands of MyHC loading controls. kD indicates protein molecular weight. Scale bar, 100 μm . Uncropped Western blots with Del-Cor., pEx-Cor., Dup-Cor., and other single colonies are presented in fig. S5.

Rather, patient mutations can be grouped such that skipping of individual exons can restore dystrophin expression in large numbers of patients. In this proof-of-concept study, our optimized myoediting approach using only one guide RNA efficiently restored the *DMD* open reading frame in a wide spectrum of mutation types, including large deletions, point mutations, and duplications, which cover most of the DMD population. The potential power of this approach lies in its simplicity and efficiency. Even relatively large and complex deletions can be corrected by a single cut in the DNA sequence that eliminates a splice acceptor or donor site without the requirement for multiple guide RNAs to direct simultaneous cutting at distant sites with ligation of DNA ends. Although exon-skipping mainly converts DMD to milder BMD, for a subset of patients with duplication or pseudo-exon mutations, myoediting can eliminate the mutations and restore the production of normal dystrophin protein, as we have shown in this study for pEx and Dup

mutations. Wojtal *et al.* (20) showed similar results for the removal of the duplication of exons 18 to 30 in DMD myotubes.

Dilated cardiomyopathy, characterized by contractile dysfunction and ventricular chamber enlargement, is one of the main causes of death in DMD patients. However, because of the marked interspecies differences in cardiac physiology and anatomy, as well as the natural history of the disease, the shortened longevity of these animals (~2 years), and the small size of their hearts (1/3000 the size of the human heart), cardiomyopathy is not generally observed in mouse models of DMD at the young age. To overcome limitations and shortcomings of 2D cell culture systems and small animal models, we used human iPSC-derived 3D-EHM to show that dystrophin mutations impaired cardiac contractility and sensitivity to calcium concentration. Contractile dysfunction was observed in DMD EHM, resembling the DCM clinical phenotype of DMD patients. Contractile dysfunction was partially-to-fully restored

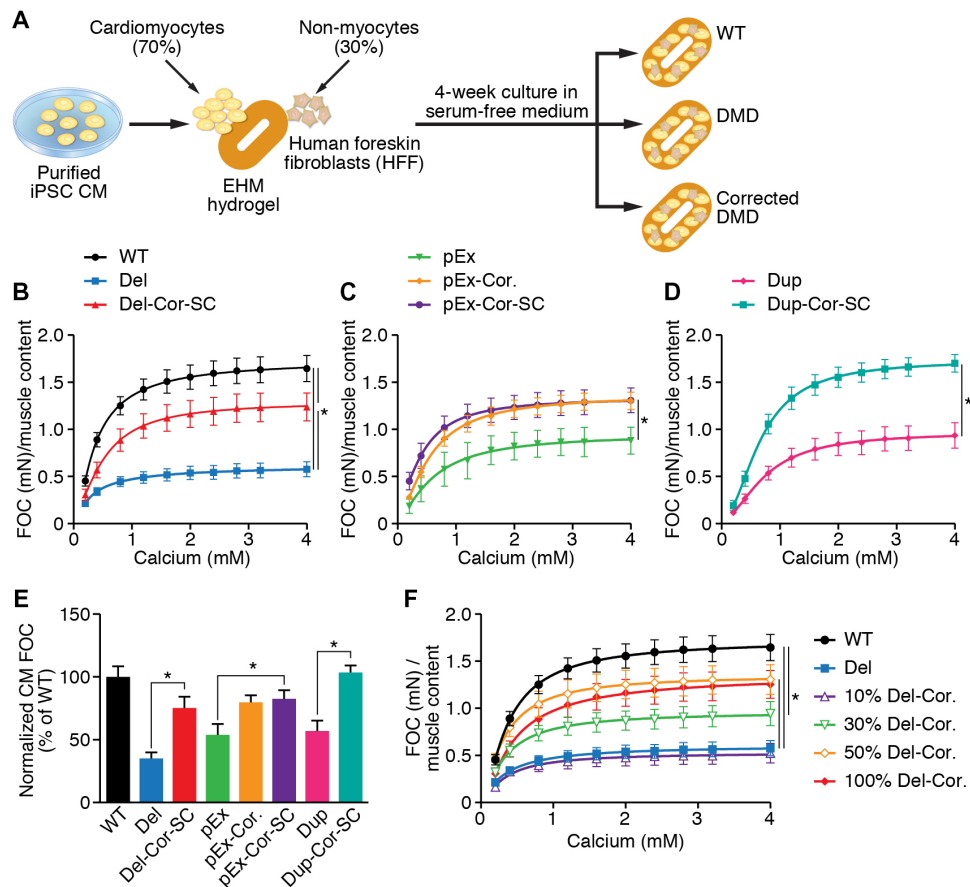


Fig. 4. Rescued DMD cardiomyocyte-derived EHM showed enhanced FOC. (A) Experimental setup for EHM preparation, culture, and analysis of contractile function. (B to D) Contractile dysfunction in DMD EHM can be rescued by myoediting. FOC normalized to muscle content of each individual EHM in response to increasing extracellular calcium concentrations; $n = 8/8/6/4/6/6/4/4$; $*P < 0.05$ by two-way analysis of variance (ANOVA) and Tukey's multiple comparison test. WT EHM data are pooled from parallel experiments with indicated DMD lines and applied to Fig. 4 (B to D). (E) Maximal cardiomyocyte FOC (at 4 mM extracellular calcium) normalized to WT. $n = 8/8/6/4/6/6/4/4$; $*P < 0.05$ by one-way ANOVA and Tukey's multiple comparison test. (F) Titration of corrected cardiomyocytes revealed that 30% of cardiomyocytes needed to be repaired to partially rescue the phenotype, and 50% of cardiomyocytes needed to be repaired to fully rescue the phenotype (100% Del-Cor.) in EHMs. WT, Del, and 100% Del-Cor. are pooled data, as displayed in Fig. 4B.

in corrected DMD EHM by myoediting. We conclude that genome editing represents a potentially effective means of eliminating the genetic cause and correcting the muscle and cardiac abnormalities associated with DMD. Our data further demonstrate that EHM serves as a suitable preclinical tool to approximate therapeutic efficiency of myoediting.

Human CRISPR clinical trials received approval in China and the United States. One key concern for the CRISPR/Cas9 system is specificity because off-target effects may cause unexpected mutations in the genome. Multiple approaches have been developed to evaluate possible off-target effects, including (i) *in silico* prediction of target sites and testing them by deep sequencing and (ii) unbiased whole-genome sequencing. In addition, several new approaches have been reported to minimize potential off-target effects and/or to improve the specificity of the CRISPR/Cas9 system, including titration of dosage of Cas9 and guide RNA (35), paired Cas9 nickases (36–38), truncated guide RNAs (39), and high-fidelity (40) or enhanced Cas9 (41). Although most studies have used *in vitro* cell culture systems, we and others did not observe off-target effects in our previous studies of germline editing and post-natal editing in mice (9, 11, 28). According to a recent study of gene editing in human preimplantation embryos, off-target mutations were also not detected in the edited genome (42). Although comprehensive

and extensive analysis of off-target effects is beyond the scope of this study, we are aware that it will eventually be important to thoroughly evaluate possible off-target effects of individual guide RNAs before potential therapeutic application.

MATERIALS AND METHODS

Plasmids

The pSpCas9(BB)-2A-GFP (PX458) plasmid containing the human codon-optimized SpCas9 gene with 2A-EGFP and the backbone of guide RNA was a gift from F. Zhang (plasmid #48138, Addgene). Cloning of guide RNA was carried out according to the Feng Zhang Lab CRISPR plasmid instructions (www.addgene.org/crispr/zhang/).

Transfection and cell sorting of human 293 cells

Cells were transfected by Lipofectamine 2000 Transfection Reagent (Thermo Fisher Scientific) according to the manufacturer's instructions, and the cells were incubated for a total of 48 to 72 hours. Cell sorting was performed by the Flow Cytometry Core Facility at University of Texas (UT) Southwestern Medical Center. Transfected cells were dissociated using trypsin-EDTA solution. The mixture was incubated for 5 min at

37°C, and 2 ml of warm Dulbecco's modified Eagle's medium supplemented with 10% fetal bovine serum was added. The resuspended cells were transferred into a 15-ml Falcon tube and gently triturated 20 times. The cells were centrifuged at 1300 rpm for 5 min at room temperature. The medium was removed, and the cells were resuspended in 500 μ l of phosphate-buffered saline (PBS) supplemented with 2% bovine serum albumin (BSA). Cells were filtered into a cell strainer tube through its mesh cap. Sorted single cells were separated into microfuge tubes into GFP⁺ and GFP⁻ cell populations.

Human iPSC maintenance, nucleofection, and differentiation

The DMD iPSC line Del was purchased from Cell Bank RIKEN BioResource Center (cell no. HPS0164). The WT iPSC line was a gift from D. Garry (University of Minnesota). Other iPSC lines (pEx and Dup) were generated and maintained by UT Southwestern Wellstone Myoeediting Core. Briefly, PBMCs obtained from DMD patients' whole blood were cultured and then reprogrammed into iPSCs using recombinant Sendai viral vectors expressing reprogramming factors (Cytotune 2.0, Life Technologies). iPSC colonies were validated by immunocytochemistry, mycoplasma testing, and teratoma formation. Human iPSCs were cultured in mTeSRTM1 medium (STEMCELL Technologies) and passaged approximately every 4 days (1:18 split ratio). One hour before nucleofection, iPSCs were treated with 10 μ M ROCK inhibitor (Y-27632) and dissociated into single cells using Accutase (Innovative Cell Technologies Inc.). Cells (1×10^6) were mixed with 5 μ g of SpCas9-2A-GFP plasmid and nucleofected using the P3 Primary Cell 4D-Nucleofector X kit (Lonza) according to manufacturer's protocol. After nucleofection, iPSCs were cultured in mTeSRTM1 medium supplemented with 10 μ M ROCK inhibitor, penicillin-streptomycin (1:100) (Thermo Fisher Scientific), and primosin (100 μ g/ml; InvivoGen). Three days after nucleofection, GFP⁺ and GFP⁻ cells were sorted by fluorescence-activated cell sorting, as described above, and subjected to PCR and T7E1 assay.

Isolation of genomic DNA from sorted cells

Protease K (20 mg/ml) was added to DirectPCR Lysis Reagent (Viagen Biotech Inc.) to a final concentration of 1 mg/ml. Cells were centrifuged at 4°C at 6000 rpm for 10 min, and the supernatant was discarded. Cell pellets kept on ice were resuspended in 50 to 100 μ l of DirectPCR/protease K solution and incubated at 55°C for >2 hours or until no clumps were observed. Crude lysates were incubated at 85°C for 30 min and then spun for 10 s. NaCl was added to a final concentration of 250 mM, followed by the addition of 0.7 volumes of isopropanol to precipitate DNA. The DNA was centrifuged at 4°C at 13,000 rpm for 5 min, and the supernatant was discarded. The DNA pellet was washed with 1 ml of 70% EtOH and dissolved in water. The DNA concentration was measured using a NanoDrop instrument (Thermo Fisher Scientific).

Amplifying targeted genomic regions by PCR

PCR assays contained 2 μ l of GoTaq polymerase (Promega), 20 μ l of 5 \times green GoTaq reaction buffer, 8 μ l of 25 mM MgCl₂, 2 μ l of 10 μ M primer, 2 μ l of 10 mM deoxynucleotide triphosphate, 8 μ l of genomic DNA, and double-distilled H₂O (ddH₂O) to 100 μ l. PCR conditions were as follows: 94°C for 2 min, 32 \times (94°C for 15 s, 59°C for 30 s, and 72°C for 1 min), 72°C for 7 min, and then held at 4°C. PCR products were analyzed by 2% agarose gel electrophoresis and purified from the gel using the QIAquick PCR Purification kit (Qiagen) for direct sequencing. These PCR products were subcloned into pCRII-TOPO vector

(Invitrogen) according to the manufacturer's instructions. Individual clones were picked, and the DNA was sequenced.

T7E1 analysis of PCR products

Mismatched duplex DNA was obtained by denaturation/renaturation of 25 μ l of the genomic PCR samples using the following conditions: 95°C for 10 min, 95° to 85°C (−2.0°C/s), 85°C for 1 min, 85° to 75°C (−0.3°C/s), 75°C for 1 min, 75° to 65°C (−0.3°C/s), 65°C for 1 min, 65° to 55°C (−0.3°C/s), 55°C for 1 min, 55° to 45°C (−0.3°C/s), 45°C for 1 min, 45° to 35°C (−0.3°C/s), 35°C for 1 min, 35° to 25°C (−0.3°C/s), 25°C for 1 min, and then held at 4°C.

Following denaturation/renaturation, the following was added to the samples: 3 μ l of 10 \times NEBuffer 2, 0.3 μ l of T7E1 (New England Biolabs), and ddH₂O to 30 μ l. Digested reactions were incubated for 1 hour at 37°C. Undigested PCR samples and T7E1-digested PCR products were analyzed by 2% agarose gel electrophoresis.

Whole-genome sequencing

Whole-genome sequencing was performed by submitting the blood samples to Novogene Corporation. Purified genomic DNA (1.0 μ g) was used as input material for the DNA sample preparation. Sequencing libraries were generated using TruSeq Nano DNA HT Sample Preparation kit (Illumina) following the manufacturer's instructions. Briefly, the DNA sample was fragmented by sonication to a size of 350 bp. The DNA fragments were end-polished, A-tailed, and ligated with the full-length adapter for Illumina sequencing with further PCR amplification. The libraries were sequenced on an Illumina sequencing platform, and paired-end reads were generated.

Isolation of RNA

RNA was isolated from cells using TRIzol RNA isolation reagent (Thermo Fisher Scientific) according to the manufacturer's instructions.

Cardiomyocyte differentiation and purification

iPSCs were adapted and maintained in TESR-E8 (STEMCELL Technologies) on 1:120 Matrigel in PBS-coated plates and passaged using EDTA solution (Versene, Thermo Fisher Scientific) twice weekly. For cardiac differentiation, iPSCs were plated at 5×10^4 to 1×10^5 cells/cm² and induced with RPMI, 2% B27, 200 μ M L-ascorbic acid-2-phosphate sesquimagnesium salt hydrate (Asc; Sigma-Aldrich), activin A (9 ng/ml; R&D Systems), BMP4 (5 ng/ml; R&D Systems), 1 μ M CHIR99021 (Stemgent), and FGF-2 (5 ng/ml; Miltenyi Biotec) for 3 days; following another wash with RPMI medium, cells were cultured from days 4 to 13 with 5 μ M IWP4 (Stemgent) in RPMI supplemented with 2% B27 and 200 μ M Asc (32). Cardiomyocytes were metabolically purified by glucose deprivation (43) from days 13 to 17 in glucose-free RPMI (Thermo Fisher Scientific) with 2.2 mM sodium lactate (Sigma-Aldrich), 100 μ M β -mercaptoethanol (Sigma-Aldrich), penicillin (100 U/ml), and streptomycin (100 μ g/ml). Cardiomyocyte purity was $92 \pm 2\%$ from 15 independent differentiation runs (one to three for each cell line).

EHM generation

To generate defined, serum-free EHM, purified cardiomyocytes were mixed with HFFs (American Type Culture Collection) at a 70%:30% ratio. The cell mixture was reconstituted in a mixture of pH-neutralized medical-grade bovine collagen (0.4 mg per EHM; LLC Collagen Solutions) and concentrated serum-free medium [2 \times RPMI, 8% B27 without insulin, penicillin (200 U/ml), and streptomycin (200 μ g/ml)] and cultured for 3 days in Iscove medium with 4% B27 without insulin, 1%

nonessential amino acids, 2 mM glutamine, 300 μ M ascorbic acid, IGF1 (100 ng/ml; AF-100-11), FGF-2 (10 ng/ml; AF-100-18B), VEGF165 (5 ng/ml; AF-100-20), TGF- β 1 (5 ng/ml; AF-100-21C; all growth factors are from PeproTech), penicillin (100 U/ml), and streptomycin (100 μ g/ml) (32). After a 3-day condensation period, EHM were transferred to flexible holders to support auxotonic contractions. Analysis was carried out after a total EHM culture period of 4 weeks.

Analysis of contractile function

Contraction experiments were performed under isometric conditions in organ baths at 37°C in gassed (5% CO₂/95% O₂) Tyrode's solution (containing 120 mM NaCl, 1 mM MgCl₂, 0.2 mM CaCl₂, 5.4 mM KCl, 22.6 mM NaHCO₃, 4.2 mM NaH₂PO₄, 5.6 mM glucose, and 0.56 mM ascorbate). EHM were electrically stimulated at 1.5 Hz with 5-ms square pulses of 200 mA. EHMs were mechanically stretched at intervals of 125 μ m until the maximum systolic force amplitude (FOC) was observed according to the Frank-Starling law. Responses to increasing extracellular calcium (0.2 to 4 mM) were investigated to determine maximal inotropic capacity. Where indicated, forces were normalized to muscle content (sarcomeric α -actinin-positive cell content, as determined by flow cytometry).

Flow cytometry of EHM-derived cells

Single-cell suspensions of EHM were prepared as described previously (32) and fixed in 70% ice-cold ethanol. Fixed cells were stained with Hoechst 3342 (10 μ g/ml; Life Technologies) to exclude cell doublets. Cardiomyocytes were identified by sarcomeric α -actinin staining (clone EA-53, Sigma-Aldrich). Cells were run on a LSRII SORP cytometer (BD Biosciences) and analyzed using the DIVA software. At least 10,000 events were analyzed per sample.

Immunostaining

iPSC-derived cardiomyocytes were fixed with acetone and subjected to immunostaining, as described previously (25). Fixed cardiomyocytes were blocked with serum cocktail (2% normal horse serum/2% normal donkey serum/0.2% BSA/PBS), and incubated with dystrophin antibody (1:800; MANDYS8, Sigma-Aldrich) and troponin-I antibody (1:200; H170, Santa Cruz Biotechnology) in 0.2% BSA/PBS. Following overnight incubation at 4°C, they were incubated with secondary antibodies [biotinylated horse anti-mouse immunoglobulin G (IgG) (1:200; Vector Laboratories) and fluorescein-conjugated donkey anti-rabbit IgG (1:50; Jackson ImmunoResearch)] for 1 hour. Nuclei were counterstained with Hoechst 33342 (Molecular Probes).

EHM cryosections to be immunostained were thawed, further air-dried, and fixed in cold acetone (10 min at -20°C). Sections were briefly equilibrated in PBS (pH 7.3) and then blocked for 1 hour with serum cocktail (2% normal horse serum/2% normal donkey serum/0.2% BSA/PBS). Blocking cocktail was decanted, and dystrophin/troponin primary antibody cocktail [mouse anti-dystrophin, MANDYS8 (1:800; Sigma-Aldrich) and rabbit anti-troponin-I (1:200; H170, Santa Cruz Biotechnology)] in 0.2% BSA/PBS was applied without intervening wash. Following overnight incubation at 4°C, unbound primary antibodies were removed with PBS washes, and sections were probed for 1 hour with secondary antibodies [biotinylated horse anti-mouse IgG (1:200; Vector Laboratories) and rhodamine donkey anti-rabbit IgG (1:50; Jackson ImmunoResearch)] diluted in 0.2% BSA/PBS. Unbound secondary antibodies were removed with PBS washes, and final dystrophin labeling was carried out with a 10-min incubation of the sections with fluorescein-avidin-DCS (1:60; Vector Laboratories) diluted in PBS.

Unbound rhodamine was removed with PBS washes, nuclei were counterstained with Hoechst 33342 (2 μ g/ml; Molecular Probes), and slides were coverslipped with Vectashield (Vector Laboratories).

Western blot analysis

Western blot analysis for human iPSC-derived cardiomyocytes was performed, as described previously (25), using antibodies to dystrophin (ab15277, Abcam; D8168, Sigma-Aldrich), glyceraldehyde-3-phosphate dehydrogenase (MAB374, Millipore), and cardiac myosin heavy chain (ab50967, Abcam). Goat anti-mouse and goat anti-rabbit horseradish peroxidase-conjugated secondary antibodies (Bio-Rad) were used for described experiments.

SUPPLEMENTARY MATERIALS

Supplementary material for this article is available at <http://advances.sciencemag.org/cgi/content/full/4/1/eaap9004/DC1>

- fig. S1. Genome editing of *DMD* top 12 exons by CRISPR/Cas9.
- fig. S2. Correction of a large deletion mutation (Del. Ex47 to Ex50) in *DMD* iPSCs and iPSC-derived cardiomyocytes.
- fig. S3. Correction of a pseudo-exon mutation (pEx47A) in *DMD* iPSCs and iPSC-derived cardiomyocytes.
- fig. S4. Correction of a large duplication mutation (Dup. Ex55 to Ex59) in *DMD* iPSCs and iPSC-derived cardiomyocytes.
- fig. S5. Dystrophin protein expression rescued by myoediting.
- fig. S6. Cardiomyocyte content and structure in myoedited EHM.
- table S1. Sequence of primers for top 12 exons.
- table S2. Sequence of primers for *DMD* iPSCs.
- table S3. DNA sequence of corrected iPSC single clones.
- movie S1. WT iPSC-derived 3D-EHM on flexible holders.
- movie S2. Uncorrected Del iPSC-derived 3D-EHM on flexible holders.
- movie S3. Del-Cor-SC iPSC-derived 3D-EHM on flexible holders.
- movie S4. Uncorrected pEx iPSC-derived 3D-EHM on flexible holders.
- movie S5. pEx-Cor. iPSC-derived 3D-EHM on flexible holders.
- movie S6. pEx-Cor-SC iPSC-derived 3D-EHM on flexible holders.
- movie S7. Uncorrected Dup iPSC-derived 3D-EHM on flexible holders.
- movie S8. Dup-Cor-SC iPSC-derived 3D-EHM on flexible holders.

REFERENCES AND NOTES

1. J. R. Mendell, C. Shilling, N. D. Leslie, K. M. Flanigan, R. al-Dahhak, J. Gastier-Foster, K. Kneile, D. M. Dunn, B. Duval, A. Aoyagi, C. Hamil, M. Mahmoud, K. Roush, L. Bird, C. Rankin, H. Lilly, N. Street, R. Chandrasekar, R. B. Weiss, Evidence-based path to newborn screening for Duchenne muscular dystrophy. *Ann. Neurol.* **71**, 304–313 (2012).
2. R. J. Fairclough, M. J. Wood, K. E. Davies, Therapy for Duchenne muscular dystrophy: Renewed optimism from genetic approaches. *Nat. Rev. Genet.* **14**, 373–378 (2013).
3. A. Fayssol, O. Nardi, D. Orlikowski, D. Annane, Cardiomyopathy in Duchenne muscular dystrophy: Pathogenesis and therapeutics. *Heart Fail. Rev.* **15**, 103–107 (2010).
4. M. Jinek, K. Chylinski, I. Fonfara, M. Hauer, J. A. Doudna, E. Charpentier, A programmable dual-RNA-guided DNA endonuclease in adaptive bacterial immunity. *Science* **337**, 816–821 (2012).
5. L. Cong, F. A. Ran, D. Cox, S. Lin, R. Barretto, N. Habib, P. D. Hsu, X. Wu, W. Jiang, L. A. Marraffini, F. Zhang, Multiplex genome engineering using CRISPR/Cas systems. *Science* **339**, 819–823 (2013).
6. P. Mali, L. Yang, K. M. Esvelt, J. Aach, M. Guell, J. E. DiCarlo, J. E. Norville, G. M. Church, RNA-guided human genome engineering via Cas9. *Science* **339**, 823–826 (2013).
7. B. Zetsche, B. Zetsche, J. S. Gootenberg, O. O. Abudayyeh, I. M. Slaymaker, K. S. Makarova, P. Essletzbichler, S. E. Volz, J. Joung, J. der Oost, A. Regev, E. V. Koonin, F. Zhang, Cpfl1 is a single RNA-guided endonuclease of a class 2 CRISPR-Cas system. *Cell* **163**, 759–771 (2015).
8. L. S. Symington, J. Gautier, Double-strand break end resection and repair pathway choice. *Annu. Rev. Genet.* **45**, 247–271 (2011).
9. C. Long, J. R. McAnally, J. M. Shelton, A. A. Mireault, R. Bassel-Duby, E. N. Olson, Prevention of muscular dystrophy in mice by CRISPR/Cas9-mediated editing of germline DNA. *Science* **345**, 1184–1188 (2014).
10. P. Zhu, F. Wu, J. Mosenson, H. Zhang, T.-C. He, W.-S. Wu, CRISPR/Cas9-mediated genome editing corrects dystrophin mutation in skeletal muscle stem cells in a mouse model of muscle dystrophy. *Mol. Ther. Nucleic Acids* **7**, 31–41 (2017).

11. C. Long, C. Long, L. Amoasii, A. A. Mireault, J. R. McAnally, H. Li, E. Sanchez-Ortiz, S. Bhattacharyya, J. M. Shelton, R. Bassel-Duby, E. N. Olson, Postnatal genome editing partially restores dystrophin expression in a mouse model of muscular dystrophy. *Science* **351**, 400–403 (2016).
12. C. E. Nelson, C. H. Hakim, D. G. Ousterout, P. I. Thakore, E. A. Moreb, R. M. Castellanos Rivera, S. Madhavan, X. Pan, F. A. Ran, W. X. Yan, A. Asokan, F. Zhang, D. Duan, C. A. Gersbach, In vivo genome editing improves muscle function in a mouse model of Duchenne muscular dystrophy. *Science* **351**, 403–407 (2016).
13. M. Tabebordbar, K. Zhu, J. K. W. Cheng, W. L. Chew, J. J. Widrick, W. X. Yan, C. Maesner, E. Y. Wu, R. Xiao, F. A. Ran, L. Cong, F. Zhang, L. H. Vandenberghe, G. M. Church, A. J. Wagers, In vivo gene editing in dystrophic mouse muscle and muscle stem cells. *Science* **351**, 407–411 (2016).
14. A. Aartsma-Rus, Overview on DMD exon skipping. *Methods Mol. Biol.* **867**, 97–116 (2012).
15. V. Kyrychenko, S. Kyrychenko, M. Tiburcy, J. M. Shelton, C. Long, J. W. Schneider, W.-H. Zimmermann, R. Bassel-Duby, E. N. Olson, Functional correction of dystrophin actin binding domain mutations by genome editing. *JCI Insight* **2**, e95918 (2017).
16. C. S. Young, M. R. Hicks, N. V. Ermolova, H. Nakano, M. Jan, S. Younesi, S. Karumbayaram, C. Kumagai-Cresse, D. Wang, J. A. Zack, D. B. Kohn, A. Nakano, S. F. Nelson, M. C. Miceli, M. J. Spencer, A. D. Pyle, A single CRISPR-Cas9 deletion strategy that targets the majority of DMD patients restores dystrophin function in hiPSC-derived muscle cells. *Cell Stem Cell* **18**, 533–540 (2016).
17. D. G. Ousterout, A. M. Kabadi, P. I. Thakore, W. H. Majoros, T. E. Reddy, C. A. Gersbach, Multiplex CRISPR/Cas9-based genome editing for correction of dystrophin mutations that cause Duchenne muscular dystrophy. *Nat. Commun.* **6**, 6244 (2015).
18. H. L. Li, N. Fujimoto, N. Sasakawa, S. Shirai, T. Ohkame, T. Sakuma, M. Tanaka, N. Amano, A. Watanabe, H. Sakurai, T. Yamamoto, S. Yamanaka, A. Hotta, Precise correction of the dystrophin gene in duchenne muscular dystrophy patient induced pluripotent stem cells by TALEN and CRISPR-Cas9. *Stem Cell Reports* **4**, 143–154 (2015).
19. L. Xu, K. H. Park, L. Zhao, J. Xu, M. El Refaey, Y. Gao, H. Zhu, J. Ma, R. Han, CRISPR-mediated genome editing restores dystrophin expression and function in *mdx* mice. *Mol. Ther.* **24**, 564–569 (2016).
20. D. Wojtal, D. U. Kemaladewi, Z. Malam, S. Abdullah, T. W. Wong, E. Hyatt, Z. Baghestani, S. Pereira, J. Stavropoulos, V. Mouly, K. Mamchaoui, F. Muntoni, T. Voit, H. D. Gonorazky, J. J. Dowling, M. D. Wilson, R. Mendoza-Londono, E. A. Ivakine, R. D. Cohn, Spell checking nature: Versatility of CRISPR/Cas9 for developing treatments for inherited disorders. *Am. J. Hum. Genet.* **98**, 90–101 (2016).
21. I. Maggio, J. Liu, J. M. Janssen, X. Chen, M. A. F. V. Gonçalves, Adenoviral vectors encoding CRISPR/Cas9 multiplexes rescue dystrophin synthesis in unselected populations of DMD muscle cells. *Sci. Rep.* **6**, 37051 (2016).
22. I. Maggio, L. Stefanucci, J. M. Janssen, J. Liu, X. Chen, V. Mouly, M. A. Gonçalves, Selection-free gene repair after adenoviral vector transduction of designer nucleases: Rescue of dystrophin synthesis in DMD muscle cell populations. *Nucleic Acids Res.* **44**, 1449–1470 (2016).
23. J. P. Iyombe-Engembe, D. L. Ouellet, X. Barbeau, J. Rousseau, P. Chapdelaine, P. Lagüe, J. P. Tremblay, Efficient restoration of the dystrophin gene reading frame and protein structure in DMD myoblasts using the CinDel method. *Mol. Ther. Nucleic Acids* **5**, e283 (2016).
24. N. E. Bengtsson, J. K. Hall, G. L. Odom, M. P. Phelps, C. R. Andrus, R. David Hawkins, S. D. Hauschka, J. R. Chamberlain, J. S. Chamberlain, Muscle-specific CRISPR/Cas9 dystrophin gene editing ameliorates pathophysiology in a mouse model for Duchenne muscular dystrophy. *Nat. Commun.* **8**, 14454 (2017).
25. Y. Zhang, C. Long, H. Li, J. R. McAnally, K. K. Baskin, J. M. Shelton, R. Bassel-Duby, E. N. Olson, CRISPR-Cpf1 correction of muscular dystrophy mutations in human cardiomyocytes and mice. *Sci. Adv.* **3**, e1602814 (2017).
26. A. Lattanzi, S. Duguez, A. Moiani, A. Izmiryan, E. Barbon, S. Martin, K. Mamchaoui, V. Mouly, F. Bernardi, F. Mavilio, M. Bovolenta, Correction of the Exon 2 Duplication in DMD Myoblasts by a Single CRISPR/Cas9 System. *Mol. Ther. Nucleic Acids* **7**, 11–19 (2017).
27. M. El Refaey, L. Xu, Y. Gao, B. D. Canan, T. M. A. Adesanya, S. C. Warner, K. Akagi, D. E. Symer, P. J. Mohler, J. Ma, P. M. L. Janssen, R. Han, In vivo genome editing restores dystrophin expression and cardiac function in dystrophic mice. *Circ. Res.* **121**, 923–929 (2017).
28. L. Amoasii, C. Long, H. Li, A. A. Mireault, J. M. Shelton, E. Sanchez-Ortiz, J. R. McAnally, S. Bhattacharyya, F. Schmidt, D. Grimm, S. D. Hauschka, R. Bassel-Duby, E. N. Olson, Single-cut genome editing restores dystrophin expression in a new mouse model of muscular dystrophy. *Sci. Transl. Med.* **9**, eaan8081 (2017).
29. A. Aartsma-Rus, I. B. Ginjaar, K. Bushby, The importance of genetic diagnosis for Duchenne muscular dystrophy. *J. Med. Genet.* **53**, 145–151 (2016).
30. A. Aartsma-Rus, I. Fokkema, J. Verschuuren, I. Ginjaar, J. van Deutekom, G. J. van Ommen, J. T. den Dunnen, Theoretic applicability of antisense-mediated exon skipping for Duchenne muscular dystrophy mutations. *Hum. Mutat.* **30**, 293–299 (2009).
31. H. G. Lidov, S. Selig, L. M. Kunkel, Dp140: A novel 140 kDa CNS transcript from the dystrophin locus. *Hum. Mol. Genet.* **4**, 329–335 (1995).
32. M. Tiburcy, J. E. Hudson, P. Balfanz, S. Schlick, T. Meyer, M.-L. Chang Liao, E. Levent, F. Raad, S. Zeidler, E. Wingender, J. Riegler, M. Wang, J. D. Gold, I. Kehat, E. Wettwer, U. Ravens, P. Dierickx, L. W. van Laake, M. J. Goumans, S. Khadjeh, K. Toischer, G. Hasenfuss, L. A. Couture, A. Unger, W. A. Linke, T. Araki, B. Neel, G. Keller, L. Gepstein, J. C. Wu, W. H. Zimmermann, Defined engineered human myocardium with advanced maturation for applications in heart failure modeling and repair. *Circulation* **135**, 1832–1847 (2017).
33. O. L. Gurvich, T. M. Tuohy, M. T. Howard, R. S. Finkel, L. Medne, C. B. Anderson, R. B. Weiss, S. D. Wilton, K. M. Flanigan, DMD pseudoexon mutations: Splicing efficiency, phenotype, and potential therapy. *Ann. Neurol.* **63**, 81–89 (2008).
34. B. Bostick, Y. Yue, C. Long, D. Duan, Prevention of dystrophin-deficient cardiomyopathy in twenty-one-month-old carrier mice by mosaic dystrophin expression or complementary dystrophin/utrophin expression. *Circ. Res.* **102**, 121–130 (2008).
35. P. D. Hsu, D. A. Scott, J. A. Weinstein, F. A. Ran, S. Konermann, V. Agarwala, Y. Li, E. J. Fine, X. Wu, O. Shalem, T. J. Cradick, L. A. Marraffini, G. Bao, F. Zhang, DNA targeting specificity of RNA-guided Cas9 nucleases. *Nat. Biotechnol.* **31**, 827–832 (2013).
36. P. Mali, J. Aach, P. B. Stranges, K. M. Esvelt, M. Moosburner, S. Kosuri, L. Yang, G. M. Church, CAS9 transcriptional activators for target specificity screening and paired nickases for cooperative genome engineering. *Nat. Biotechnol.* **31**, 833–838 (2013).
37. B. Shen, W. Zhang, J. Zhang, J. Zhou, J. Wang, L. Chen, L. Wang, A. Hodgkins, V. Iyer, X. Huang, W. C. Skarnes, Efficient genome modification by CRISPR-Cas9 nickase with minimal off-target effects. *Nat. Methods* **11**, 399–402 (2014).
38. F. A. Ran, P. D. Hsu, C. Y. Lin, J. S. Gootenberg, S. Konermann, A. E. Trevino, D. A. Scott, A. Inoue, S. Matoba, Y. Zhang, F. Zhang, Double nicking by RNA-guided CRISPR Cas9 for enhanced genome editing specificity. *Cell* **154**, 1380–1389 (2013).
39. Y. Fu, J. D. Sander, R. Reyon, V. M. Cascio, J. K. Joung, Improving CRISPR-Cas nuclease specificity using truncated guide RNAs. *Nat. Biotechnol.* **32**, 279–284 (2014).
40. B. P. Kleinstiver, V. Pattanayak, S. Q. MS Prew, N. T. N. Tsai, Z. Zheng, J. K. Joung, High-fidelity CRISPR-Cas9 nucleases with no detectable genome-wide off-target effects. *Nature* **529**, 490–495 (2016).
41. I. M. Slaymaker, L. Gao, B. Zetsche, D. A. Scott, W. X. Yan, F. Zhang, Rationally engineered Cas9 nucleases with improved specificity. *Science* **351**, 84–88 (2016).
42. H. Ma, N. Marti-Gutierrez, S. W. Park, J. Wu, Y. Lee, K. Suzuki, A. Koski, D. Ji, T. Hayama, R. Ahmed, H. Darby, C. Van Dyken, Y. Li, E. Kang, A. R. Park, D. Kim, S. T. Kim, J. Gong, Y. Gu, X. Xu, D. Battaglia, S. A. Krieg, D. M. Lee, D. H. Wu, D. P. Wolf, S. B. Heitner, J. C. I. Belmonte, P. Amato, J. S. Kim, S. Kaul, S. Mitalipov, Correction of a pathogenic gene mutation in human embryos. *Nature* **548**, 413–419 (2017).
43. S. Tohyama, F. Hattori, M. Sano, T. Hishiki, Y. Nagahata, T. Matsuura, H. Hashimoto, T. Suzuki, H. Yamashita, Y. Satoh, T. Egashira, T. Seki, N. Muraoka, H. Yamakawa, Y. Ohgino, T. Tanaka, M. Yoichi, S. Yuasa, M. Murata, M. Suematsu, K. Fukuda, Distinct metabolic flow enables large-scale purification of mouse and human pluripotent stem cell-derived cardiomyocytes. *Cell Stem Cell* **12**, 127–137 (2013).

Acknowledgments: We thank J. Cabrera for the assistance with graphics. We thank A. Mireault and S. Bhattacharyya for the cloning and sequencing of guide RNAs. We thank D. Reher for differentiating the iPSC lines. **Funding:** This work was supported by grants from the NIH (HL-130253, HL-077439, DK-099653, and AR-067294), a Senator Paul D. Wellstone Muscular Dystrophy Cooperative Research Center grant (U54 HD-087351), Parent Project Muscular Dystrophy, and the Robert A. Welch Foundation (grant 1-0025 to E.N.O.). M.T., N.Y.L., and W.-H.Z. are supported by the DZHK (German Center for Cardiovascular Research), the German Federal Ministry for Science and Education [BMBF FKZ 13GW0007A (CIRM-ET3)], the German Research Foundation (DFG ZI 708/7-1, 8-1, 10-1; SFB 937 TP18, SFB 1002 TPs B03, C04, S1; IRTG 1816 RP12), and the Fondation Leducq. **Author contributions:** C.L., H.L., M.T., W.-H.Z., R.B.-D., J.W.S., and E.N.O. designed the project. C.L., H.L., M.T., C.R.-C., V.K. H.Z., Y.Z., Y.-L.M., J.M.S., P.P.A.M., and N.Y.L. performed the experiments. C.L., R.B.-D., J.W.S., and E.N.O. wrote and edited the manuscript. **Competing interests:** R.B.-D. and E.N.O. are consultants for Exonics Therapeutics. M.T. is a consultant and W.-H.Z. is a founder of myriamed GmbH. E.N.O., C.L., J.M.S. and R.B.-D. are listed on a patent related to this work (application no. US 14/823,563, filed 11 August 2015). All other authors declare that they have no competing interests. **Data and materials availability:** All data needed to evaluate the conclusions in the paper are present in the paper and/or the Supplementary Materials. Additional data related to this paper may be requested from the authors.

Submitted 7 September 2017

Accepted 28 December 2017

Published 31 January 2018

10.1126/sciadv.aap9004

Citation: C. Long, H. Li, M. Tiburcy, C. Rodriguez-Caycedo, V. Kyrychenko, H. Zhou, Y. Zhang, Y.-L. Min, J. M. Shelton, P. P. A. Mammen, N. Y. Liaw, W.-H. Zimmermann, R. Bassel-Duby, J. W. Schneider, E. N. Olson, Correction of diverse muscular dystrophy mutations in human engineered heart muscle by single-site genome editing. *Sci. Adv.* **4**, eaap9004 (2018).